Materials Research Express

Femtosecond laser fabrication of silver plasmonic structures for application as single particle SERS detectors

H Huang[1,2], A Hu[1,2,3], M Sivayoganathan[1,2], W W Duley[1,4], Z H Huang[5] and Y Zhou[1,2]

[1] Centre for Advanced Materials Joining, University of Waterloo, Ontario N2L 3G1, Canada
[2] Department of Mechanical & Mechatronics Engineering, University of Waterloo, Ontario N2L 3G1, Canada
[3] Department of Mechanical, Aerospace, Biomedical Engineering, University of Tennessee Knoxville, Knoxville TN 37996, USA
[4] Department of Physics & Astronomy, University of Waterloo, Ontario N2L 3G1, Canada
[5] School of Materials Science and Technology, China University of Geosciences, Beijing 100083, People's Republic of China
E-mail: nzhou@uwaterloo.ca

Received 4 February 2014, revised 28 March 2014
Accepted for publication 4 April 2014
Published 7 May 2014

Materials Research Express **1** (2014) 025022

doi:10.1088/2053-1591/1/2/025022

Abstract

This work demonstrates the feasibility of fabricating silver nanoparticles (NPs) into sub-micron and micron-sized core-satellite structures by exposure to femtosecond laser radiation. We find that the size and shape of these structures can be tailored by adjusting laser fluence (1.8–10.5 J cm^{-2}) and irradiation time (20–60 min), along with the concentration of NPs in aqueous solution (0.01–0.05 mM). Raman measurements of adenine molecules adsorbed on these sub-micron substrates indicate that core-satellite structures having complex shapes are effective as sensitive surface enhanced Raman spectroscopy (SERS) substrates. The sensitivity is such that these structures are potentially useful as single particle SERS substrates for bio-sensing. Finite difference time domain (FDTD) simulation results indicate that these structures can be generated by the joining of NPs in response to localized surface plasmon induced hotspots.

Keywords: femtosecond laser, silver plasmonic structure, SERS

1. Introduction

For decades, nanoparticles (NPs) have been of great interest to researchers because of their unique chemical [1], electronic [2], magnetic [3] and optical properties [4]. With the

development of plasmonics research, the surface plasmon property of NPs has been extensively studied. As reported, plasmon resonance on the surface of NPs can produce localized electromagnetic field enhancement (hotspots) and amplify the signal for optical detection via SERS [5]. A major focus of research into surface plasmon has involved the directed assembly of NPs structures for applications ranging from bio-sensing [6], to solar energy harvesting [7], and to photothermal imaging [8].

To date, a variety of chemical methods have been utilized to fabricate NPs structures. For example, Sebba *et al* [9] and Gandra *et al* [5] produced gold NPs core-satellite structures using DNA and p-aminothiophenol as molecular linkages. It was found that these structures showed large scattering activity. Choi *et al* [10] and Yoon *et al* [11] have also reported similar core-satellite structures. Recent studies have shown that necklace [4, 12–14] and chain-like [15–17] NPs structures also exhibit unique electronic and optical properties. However, chemical fabrication processes are frequently complicated and time-consuming. Alternative techniques such as those incorporating electric/magnetic field induced dipole-dipole interactions [18–20] are faster and simpler and have been widely studied, but the use of inter-NP polymer linkages can introduce instability in the plasmonic properties of the resulting structures [21].

Recently, laser assembled NPs structures have attracted much attention because they are straightforward and readily implemented. It has been demonstrated that NPs can be manipulated using laser-induced optical forces and that robust joining of NPs is facilitated by the optical electric field concentrated near hotspots between nearby NPs [22–25]. However, when a continuous-wavelength laser is used, the low laser intensities required to avoid thermal damage in the NP structures [26] result in optical forces that are weaker than those arising from van der Waals interactions [27]. Under these conditions, the resulting NPs structures are poorly constrained.

Femtosecond (fs) laser radiation is a promising alternative for the fabrication of NPs structures, as high peak intensities (10^{14}–10^{15} W cm^{-2}) are known to induce strong optical forces on NPs. Meanwhile, the limited thermal damage of associated with fs laser pulses interaction with materials [28] facilitates the fabrication of NPs structures having different geometries that can be tailored to optimize tunable plasmon properties [29]. In addition, the fabrication of NPs structures incorporating plasmonic single particles is also becoming an interesting research topic because of the emerging need for single particle SERS detection, tracking, and photothermal imaging in bio-sensing [30]. To our knowledge, the work reported here is the first study of the effectiveness of the irradiation of silver (Ag) NPs in solution with fs laser pulses as a fabrication technique for sensitive micron-sized and micron plasmonic structures that can act as single particle SERS substrates.

2. Experimental and simulation

Ag NPs with an average particle size of 50 nm were introduced into an aqueous solution of polyvinylpyrrolidone (PVP) as reported previously [31]. This solution, containing PVP coated Ag NPs, was diluted with deionized water to 0.01 and 0.05 mM before laser irradiation. 5 ml of these diluted Ag NP solutions were then placed into individual quartz cells and irradiated with focused S polarized fs laser pulses for various exposure times. This laser with pulse duration 35 fs and wavelength 800 nm at 1 kHz was manufactured by Coherent. Pulse energies of 85, 200 and 500 μJ were obtained by attenuating the beam with neutral density filters (Thorlab).

Scanning electron microscopy (SEM, LEO 1530 Zeiss, Germany) and transmission electron microscopy (TEM, JEOL-JEM-2010F) were used to analyze particle morphology. The transmittance of irradiated samples was characterized using UV-VIS-NIR spectroscopy (Shimadzu, UV-2500). SERS enhancement of sub-micron plasmonic structures deposited on cleaned Si substrates was evaluated using 10^{-3} M adenine solution as analyte, Raman signals from six spots were collected for analysis. The SERS detection limit was also evaluated by reducing the concentration of adenine solution to 10^{-5}, 10^{-7} and then 10^{-9} M. The wavelength of the laser for excitation of SERS spectra was 633 nm. Commercial FDTD software (Lumerical) was used to identify the hotspots distribution in representative sub-micron structures.

3. Results and discussion

Figure 1 shows SEM images of particles extracted from the 0.01 mM Ag NPs solution after irradiation at different fs laser pulse fluences. It is evident that Ag sub-micron structures were generated following 60 min of laser irradiation (figures 1(a), (c) and (e)), and these sub-micron structures were not observed prior to laser irradiation as the particle size in the solution before irradiation is 50 ± 10 nm. SEM images at higher magnification (figures 1(b), (d) and (f)) indicate that the surfaces of these sub-micron structures were decorated by smaller Ag NPs (higher resolution TEM images are shown later) and that the shape of the sub-micron structures depended on the pulse fluence. Figure 1(b) shows that ellipsoidal sub-micron structures were formed after irradiation at 1.8 J cm^{-2}, while cubic sub-micron structures (figure 1(d)) and other structures with highly organized features (figure 1(f)) were produced at pulse fluences of 4.2 and 10.5 J cm^{-2}, respectively. This suggests that the morphology of the sub-micron structures can be tailored by controlling the laser pulse fluence. In this context, the modification of NP particle shapes has been shown to be useful in obtaining tunable plasmonic properties [29]. It should be noted that sub-micron structures with some of these characteristics were also observed in the NP solutions irradiated at different fluences. This is probably due to the random Brownian movement of the NPs, and the non-uniform spatial distribution of laser intensity in the solution during irradiation.

To produce a higher abundance of sub-micron structures using this technique, the concentration of Ag NPs in solution was increased to 0.05 mM. Under the same irradiation conditions as at lower concentration, sub-micron structures with similar morphology were obtained (figure 2), while the size and shape of the sub-micron structures were more uniform. Figures 2(a), (b) show that Ag sub-micron structures with diameters of 450 ± 130 nm together with individual NPs were obtained after irradiation at a pulse fluence of 1.8 J cm^{-2}. The diameter of the sub-micron structures increased to 710 ± 140 nm when the pulse fluence was increased to 4.2 J cm^{-2}, and some NPs were still found in the surrounding medium (figure 2(c)). A further increase in the pulse fluence to 10.5 J cm^{-2} resulted in the transformation and enhanced joining of NPs into large micron-sized structures with diameters of 1480 ± 300 nm (figures 2(e), (f)), as well as a small number of sub-micron structures with diameters of 620 ± 100 nm (figure 2(g)). The morphology of these structures was also determined from AFM (figure 2(h)). It should be noted that there were also some NPs ranging in size from ~5 nm to 100 nm surrounding the sub-micron and micron-sized structures (figures 2(e), (f)). These NPs were likely produced by the ablation of sub-micron and micron-sized structures or they might

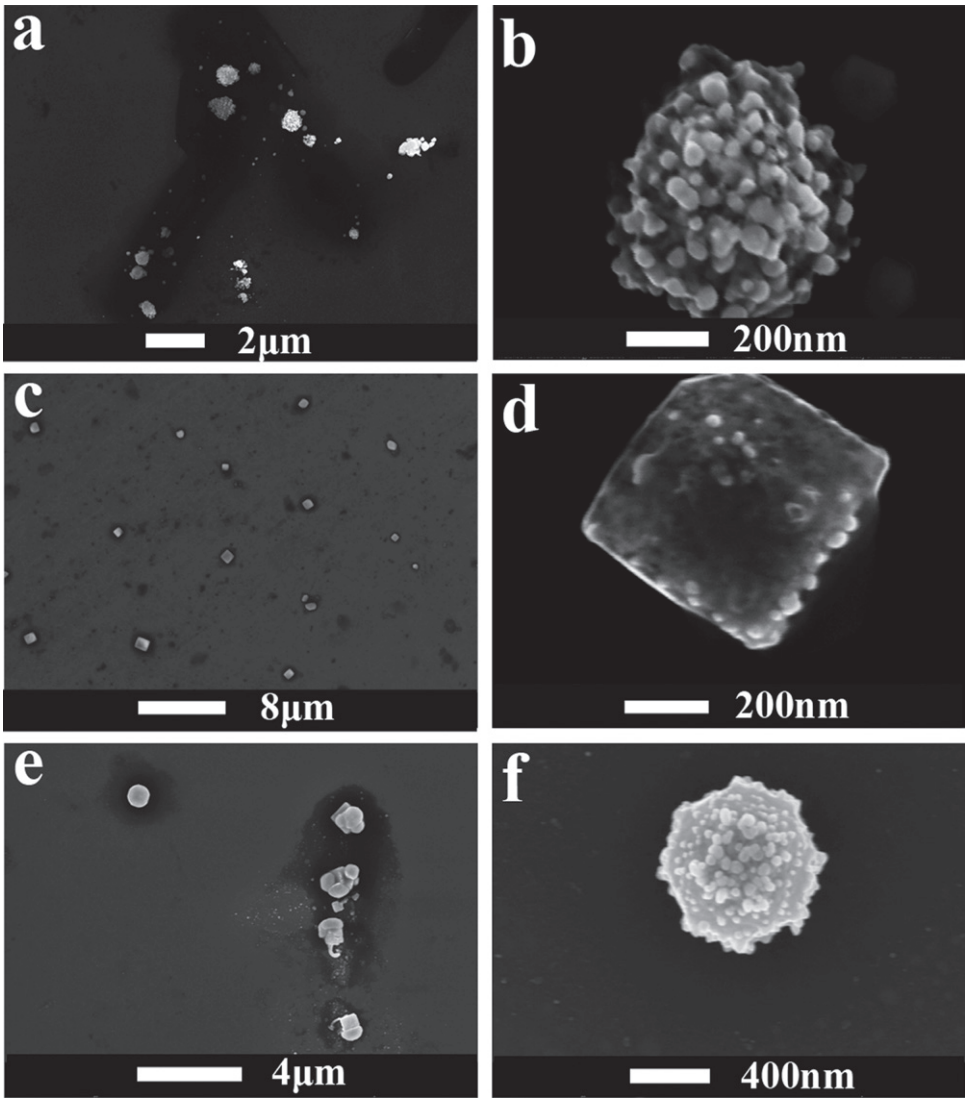

Figure 1. SEM images of sub-micron structures obtained by fs laser irradiation of 0.01 mM Ag NP solutions under different irradiation parameters; (a), (b), 1.8 J cm^{-2} for 60 min, (c), (d), 4.2 J cm^{-2} for 60 min, (e), (f), 10.5 J cm^{-2} for 60 min.

be remnants of the original NPs in the solution. Again, all the sub-micron and micron-sized structures were also decorated by smaller NPs (figures 2(b), (d), and (f)).

To determine how the sub-micron and micron-sized structures were produced, a 0.05 mM aqueous solution of Ag NPs was irradiated at a pulse fluence of 10.5 J cm^{-2} for different times. Figures 3(a)–(c) show the morphology of the particles/structures in the solution before and after laser irradiation. It can be seen (figure 3(a)) that, before irradiation, some Ag NPs were linked in networks as a result of inter-particle agglomeration, which could be due to van der Waals force, electrostatic interaction or chemical effects [32]. After 20 min irradiation, the number of Ag NPs networks has been reduced and some sub-micron particle-like structures with variable diameters begin to appear (figure 3(b)). The inset in figure 3(b) shows the morphology of the large structures, and indicates that these sub-micron structures (290 ± 100 nm) were covered

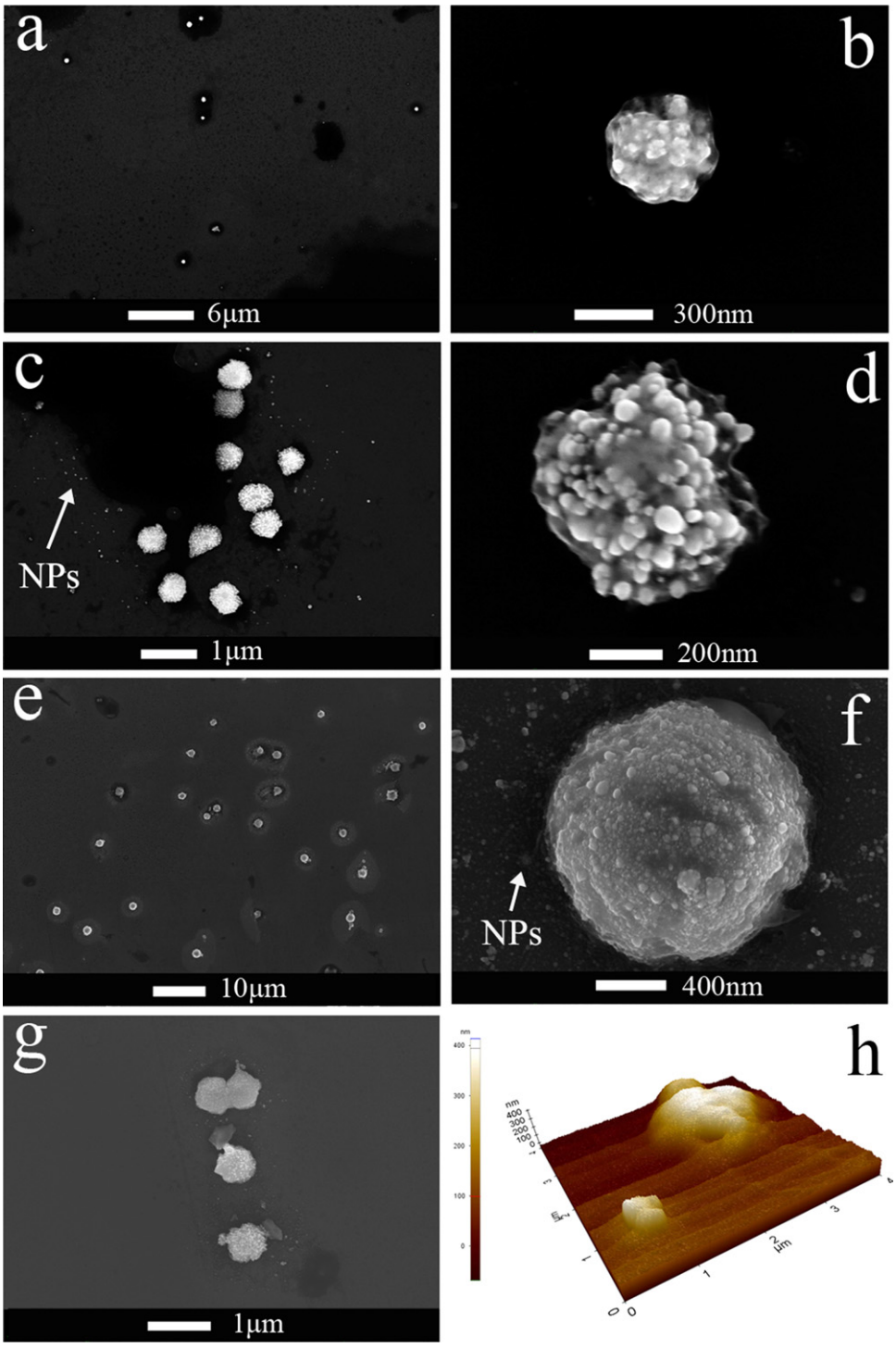

Figure 2. SEM and AFM scans of sub-micron and micron-sized structures obtained by fs laser irradiation of 0.05 mM Ag NP solutions under different irradiation parameters; (a), (b), 1.8 J cm^{-2} for 60 min, (c), (d), 4.2 J cm^{-2} for 60 min, (e), (f), (g), (h), 10.5 J cm^{-2} for 60 min.

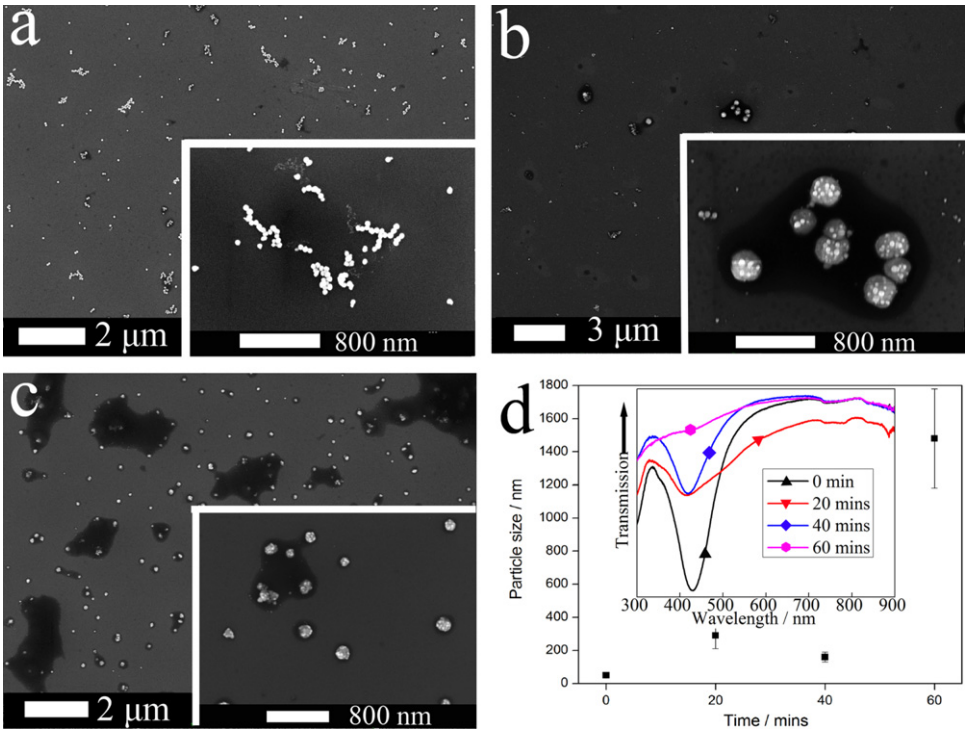

Figure 3. SEM morphologies and transmittance spectra of samples after irradiation at a pulse energy of 10.5 J cm^{-2} for different times, (a) 0 min, (b) 20 min, (c) 40 min, (d) transmittance spectra and derived particle/structure size after different irradiation times.

with many NPs as observed in the structures shown in figures 1 and 2. It is believed that these NPs decorated sub-micron structures will favor the plasmonic enhancement [33]. When the irradiation time increased to 40 min (figure 3(c)), Ag NPs were transformed into large well dispersed sub-micron structures with diameters of 160 ± 50 nm. The reduction of sub-micron structures diameter from 290 ± 100 nm to 160 ± 50 nm was attributed to the densification of the NPs structures due to local heating and welding at the hotspots [34]. After a further increase in the irradiation time to 60 min, the 160 nm sub-micron-sized structures disappeared, and 1480 nm diameter micron structures were generated (figures 2(f), (g)).

Particle/structure sizes in the solution before and after fs laser irradiation are shown in figure 3(d), which indicates a general trend that the structure size increased with the laser irradiation time. As reported previously, NPs can be attracted and joined together because of the enhanced optical force and heat generation at the hotspots [25, 35]. The diameters of the sub-micron structures will increase as more NPs are attracted to the existing sub-micron structures. In addition, it is apparent that even sub-micron structures can be combined. On the other hand, welding among NPs and sub-micron structures may reduce their diameters because of densification. Therefore, the final diameters observed reflect the interplay between these two factors, which may explain why the diameters of the sub-micron structures at 40 min were smaller than those at 20 min.

Transmittance spectra (inset in figure 3(d)) of the NPs solution before and after irradiation were also studied. These spectra show that the transmittance of the original NPs (50 ± 10 nm) was reduced at 430 nm, due to excitation of the plasmon resonance [36]. After 20 min of

irradiation, the transmittance at 430 nm increased, which can be associated with a reduction in the concentration of the original small NPs. The transmittance of the solution between 550–900 nm also decreased after 20 min irradiation, following the formation of larger particles that scatter and absorb laser radiation efficiently over this wavelength range [37]. This is consistent with the SEM observations in figure 3(b), and the observation of a scattering peak at 880 nm indicates that large particles/structures were present in the irradiated solution [38]. With an increase in the irradiation time to 40 min, the transmittance between 550 and 900 nm was increased while that at 430 nm was almost unchanged. This is probably due to the growth of NPs together with the densification of 290 ± 100 nm sub-micron structures into 160 ± 50 nm sub-micron structures with resonance wavelengths in the near infrared. After a further increase in irradiation time to 60 min, the resonance peak at 430 nm disappeared and no other resonance peaks could be seen in the spectrum, suggesting that most of the NPs have become incorporated into the sub-micron and micron-sized structures. We did not see the blue shift in the NP resonance as reported elsewhere, even though the fs laser pulses were sufficiently intense to fragment NPs [39–41]. We attribute this to the fact that only a small number of NPs were fragmented while the products of this fragmentation had a wide size distribution which broadens the plasmon resonance.

TEM images of Ag NPs after irradiation at a pulse fluence of 10.5 J cm^{-2} for 40 min are shown in figure 4. It can be seen that many Ag NPs (50 ± 10 nm) and tiny Ag NPs (5–20 nm in diameter) were collected on the surface and become joined to the larger (160 ± 50 nm) core particle, forming a core-satellite structure. These sub-micron particles further combined in some cases to form even more complex-shaped structures (figure 4(a)). The tiny NPs seen at this stage may be produced by laser induced fragmentation from the original NPs (50 ± 10 nm). The core-satellite NP structures have been reported to possess high SERS enhancement factors [5], implying that these complex-shaped structures in this work could be used for SERS detection.

HRTEM analysis shows that Ag NP (label ① in figure 4(b)) has been welded to the core particle with the Ag(111) lattice planes aligned. This NP-core particle weld morphology will enable the generation of hotspots in the neck area, resulting in the plasmonic enhancement effect. Bonding of tiny NPs to core particles via a thin layer of amorphous carbon (α-C) (indicated by dashed lines in figure 4(b)) was also observed. This bond configuration has been seen previously and was demonstrated to be also beneficial for the enhancement of SERS [36]. The SERS enhancement properties of these complex-shaped structures may also be fairly reproducible due to the narrow size distribution (5–20 nm) of the attached tiny NPs (figure 4(b)) and the robust NP-core weld strength. This is supported by the SERS analyses of the sub-micron structures on the wafer (the data were collected from six spots). As shown in figure 4(c), the sharp characteristic peaks of adenine [42, 43] at ~726 and 1325 cm^{-1} indicates that these sub-micron structures could produce high SERS enhancement. As seen in figure 3(c), the number of sub-micron structures in the Raman laser spot size (~1 μm) is small (<6), we suggest that these sub-micron structures possess the potential for single particle SERS enhancement as required for ultra-sensitive bio-sensing [30].

To assess this possibility, SERS spectra were obtained for individual Ag particle structures with sizes ~160 nm for a range of low concentration adenine solutions. Figure 5 shows that when the concentration of adenine solution was decreased from 10^{-5} to 10^{-7} and then to 10^{-9} M, the characteristic peak of adenine at ~1319 cm^{-1} gradually became undetectable. However, the spectral feature at ~735 cm^{-1} was observed although it became broader and its intensity relative to the Si peak 951 cm^{-1} decreased. This suggests that the sub-micron Ag NP

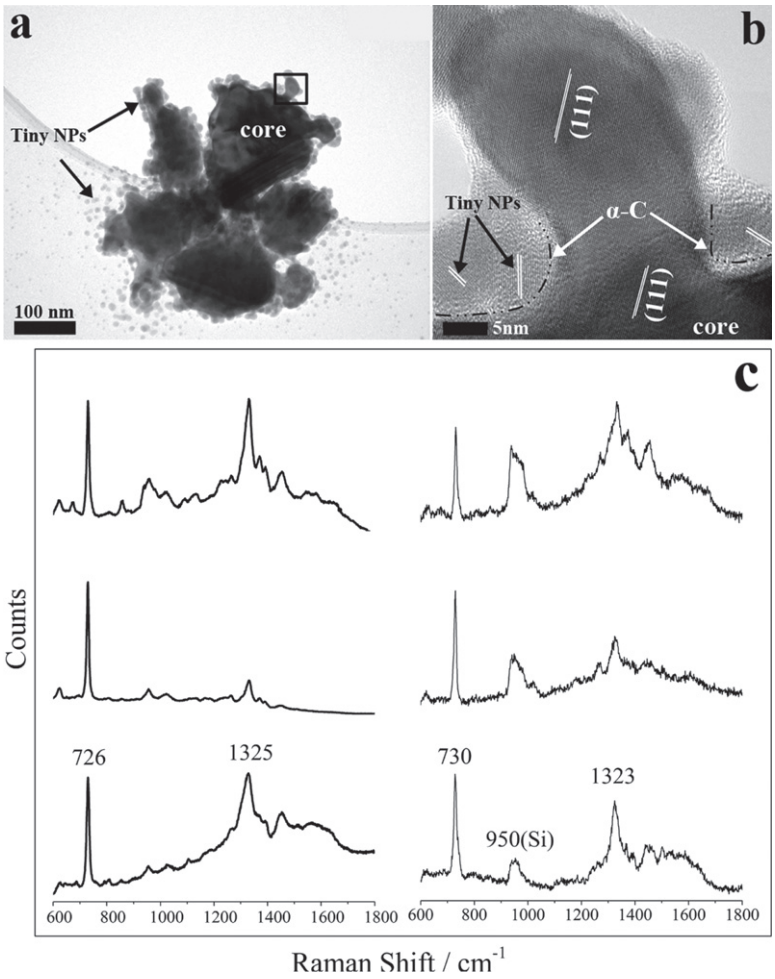

Figure 4. TEM observation SERS analyses of the sample irradiated at a fluence of 10.5 J cm^{-2} for 40 min (a) TEM image of the morphology for sub-micron structures, (b) is taken from the square area in (a). The dash lines in (b) show the positions of amorphous carbon (α-C). (c) SERS results from six sub-micron structures spots (Raman spot size is $\sim$1 μm) in the sample irradiated at fluence 10.5 J cm^{-2} for 40 min, the analyte molecule is adenine.

structures produced using fs irradiation contain a range of bonding sites having different enhancement characteristics. The activity of individual sites for SERS enhancement is reflected in the changes in the SERS spectra in figure 5 as the concentration of adenine is reduced. This observation indicates that sub-micron Ag composite structures may exhibit useful properties for the detection of low concentrations bio-molecules in solution.

As discussed above, sub-micron structures are created via the joining of NPs and are therefore related to the formation and evolution of hotspots. In these structures, the surface plasmon becomes localized, forming hotspots adjacent to the sub-micron structures. These hotspots produces two effects: one is to produce local heating [41], which promotes the joining of NPs; the other is to increase the electric field gradient between hotspots and the surrounding medium, which enhances the attraction to the nearby NPs via enhanced optical gradient force [44]. These two effects may facilitate further joining of NPs.

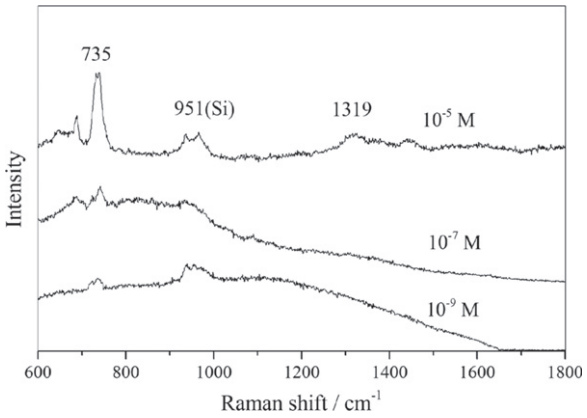

Figure 5. SERS spectra obtained under single ~160 nm Ag structures for different concentrations (10^{-5}, 10^{-7}, and 10^{-9} M) adenine solutions.

To investigate the possibility of NPs joining into the above observed structures in response to the development of hotspots, a FDTD simulation was performed. In the simulation, individual NPs in the aggregates are assumed to be 50 nm in diameter, and the bold red lines in figure 6 trace the outlines of the NPs. The simulation begins with two welded NPs with certain overlap distance (surface to surface distance) *d* which is defined in figure 6(a). As shown in figure 6(b), the initial overlap distance *d* between welded NPs is very small (~2 nm, measured from the joined NPs in the solution at fluence 10.5 J cm^{-2} for 30 s). After laser irradiations with polarization parallel to the *x* axis of the welded structure, the locations of the hotspots in the welded structure were identified (as the arrows in figure 6(c) shown). By introducing additional NPs into the hotspots where the electric field was enhanced, the distribution of the hotspots in the resulted larger welded NPs structures could be identified (figure 6(d)). With further continuous placement of NPs in hotspots, larger sized or even final joined NPs structures could be modeled (figures 6(e), (f)). It is clear that when the overlap distance was fixed to 2 nm, a 3D welded NPs structure was developed by continuously introducing additional NPs into the hotspots (figure 6(f)). As shown in figure 6(f), the 3D NPs structure (containing 32 NPs) had a diameter of ~250 nm; this is close to the observed 290 nm diameter of the structure which was obtained after fs laser irradiation at fluence 10.5 J cm^{-2} for 20 min (figure 3(d)). Then we stopped further introducing NPs in the structure and modeled the absorption spectra of the present structures.

The calculation results of the absorption cross-section show that with the increase of the number of NPs in the structure, the absorption at wavelength of 800 nm increased (figure 7). When the number of the NPs in the structure increased to 32, an absorption peak at 816 nm appeared. This is consistent with the observed peak at 880 nm in the transmittance spectra (figure 3(d)) of the fs irradiated solution at fluence 10.5 J cm^{-2} for 20 min It implies that the 290 nm sub-micron structure could be formed by hotspots-directed joining of Ag NPs through the enhanced optical gradient force. In addition, because the absorption wavelength of the structure is close to that of the incident laser, significant absorption of the laser energy will happen in the welded structure due to the excitation of SPR [41] and consequently result in the heating and densification of the welded structure. This is probably the cause for the observed densification of 290 nm sub-micron structure when the irradiation time increase from 20 min to 40 min at fluence of 10.5 J cm^{-2} (figure 3(d)).

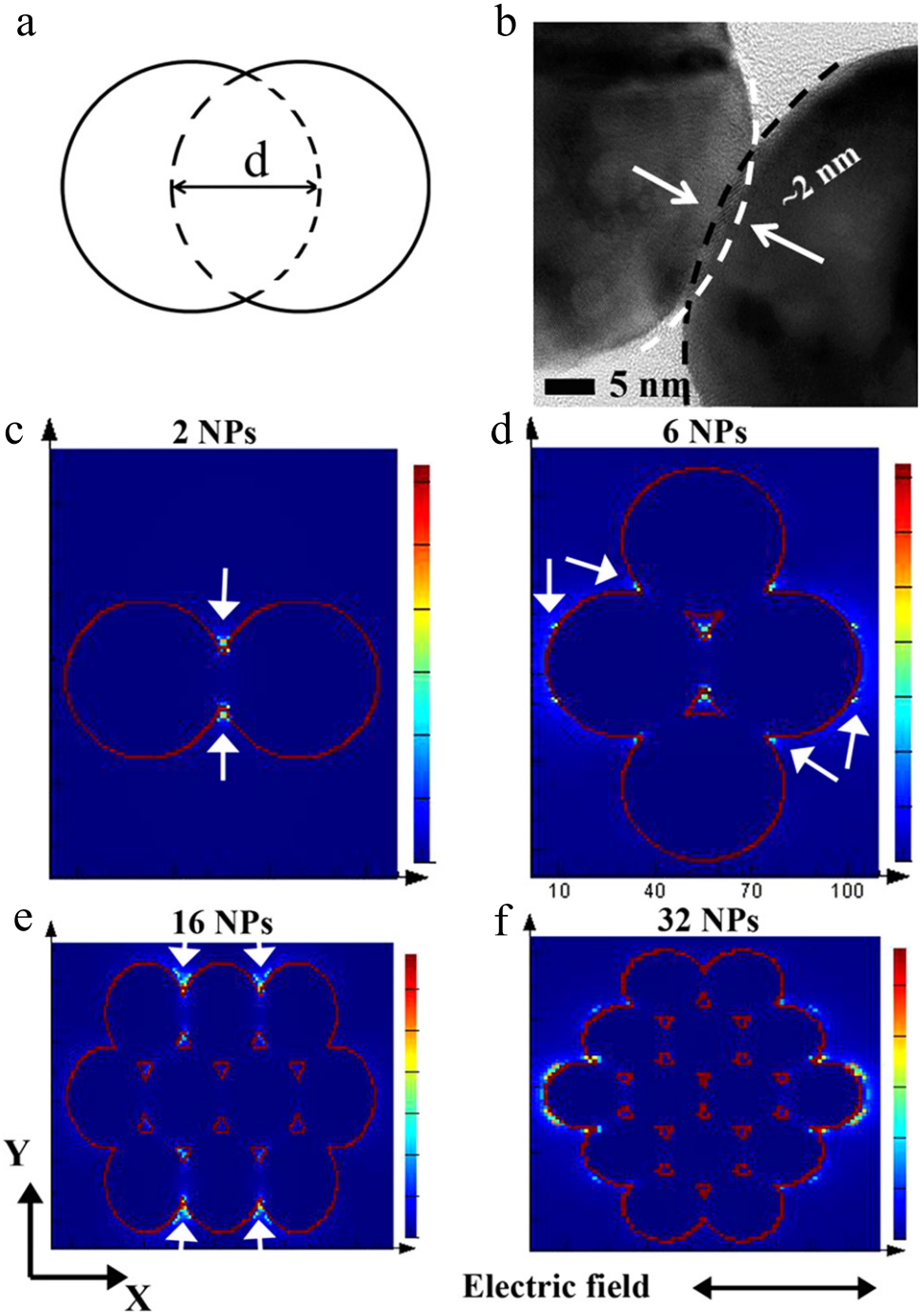

Figure 6. FDTD simulation of electric field distribution in welded NPs structures. (a) definition of overlap distance d, (b) measured overlap distance, (c)–(f) electric field distribution in structures containing 2, 6, 16 and 32 NPs, respectively. In the scale bar for the electric field, the electric field intensity increases from blue to red. The arrows in the images show the locations of the hotspots in the structures.

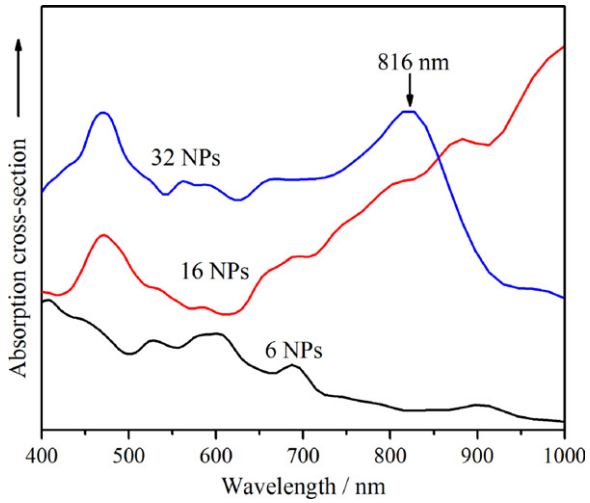

Figure 7. Calculated absorption cross-section in the structures containing different numbers of Ag NPs.

It is noted that the FDTD simulation cannot perfectly mimic fs laser joining due to complex irradiation environment in the aqueous solution and the dynamic evolution of the geometry of welded NP structure during the whole joining process. Further studies are still needed to better understand localized surface plasmon (LSP) induced joining of NPs via an enhanced the laser-induced optical gradient force.

4. Conclusions

We show here that complex-shaped core-satellite submicron and micron-sized structures can be synthesized by focusing a high intensity fs laser beam into an aqueous solution of Ag NPs. By adjusting the concentration of NPs in the solution (0.01–0.05 mM), the irradiation time (20–60 min), and the laser fluence (1.8–10.5 J cm^{-2}), we show that it is feasible to control the sizes and shape of the resulting structures. For example, at a pulse fluence of 10.5 J cm^{-2}, well dispersed 160 nm and 1480 nm particles were produced in the 0.05 mM solution after 40 and 60 min of irradiation, respectively. These complex plasmonic structures have potential applications as single particle detectors for biomolecules at low concentration. FDTD simulations indicate that the formation of these structures can be attributed to the joining of NPs which is directed by LSP induced hotspots.

Acknowledgements

The work is financially supported from the National Sciences and Engineering Research Council (NSERC) and the State Scholarship Fund of China (No. 2011640021). The authors would like to acknowledge Carmen Andrei, from the Canadian Center of Electron Microscopy at McMaster University which is supported by NSERC and other government agencies, for help in the TEM measurements, and thanks Mr Peng Peng from Department of Mechanical and Mechatronics Engineering at University of Waterloo for valuable discussions.

References

[1] Daniel M C and Astruc D 2004 *Chem. Rev.* **104** 293–346
[2] Hardman S J O *et al* 2011 *Phys. Chem. Chem. Phys.* **13** 20275–83
[3] Yurkov G Y, Fionov A S, Koksharov Y A, Kolesov V V and Gubin S P 2007 *Inorganic Mater.* **43** 834–44
[4] Zhang Y, Chen Y, Niu H and Gao M 2006 *Small* **2** 1314–9
[5] Gandra N, Abbas A, Tian L and Singamaneni S 2012 *Nano Lett.* **12** 2645–51
[6] Bruls D M *et al* 2009 *J. Lab. Chip* **9** 3504–10
[7] Thomann I, Pinaud B A, Chen Z, Clemens B M, Jaramillo T F and Brongersma M L 2011 *Nano Lett.* **11** 3440–6
[8] Boyer D, Tamarat P, Maali A, Lounis B and Orrit M 2002 *Science* **297** 1160–3
[9] Sebba D S, Mock J J, Smith D R, LaBean T H and Lazarides A A 2008 *Nano Lett.* **8** 1803–8
[10] Choi I, Song H D, Lee S, Yang Y I, Kang T and Yi J 2012 *J. Am. Chem. Soc.* **134** 12083–90
[11] Yoon J H, Lim J and Yoon S 2012 *ACS Nano* **6** 7199–208
[12] Wang C, Chen J, Talavage T and Irudayaraj J 2009 *Angew. Chem., Int. Ed.* **48** 2759–63
[13] Kane J, Inan M and Saraf R F 2010 *ACS Nano* **4** 317–23
[14] Hanisch M, Mačković M, Taccardi N, Spiecker E and Klupp R N T 2012 *Chem. Commun.* **48** 4287–9
[15] Nie Z, Fava D, Kumacheva E, Zou S, Walker G C and Rubinstein M 2007 *Nat. Mater.* **6** 609–14
[16] Wang L, Zhu Y, Xu L, Chen W, Kuang H, Liu L, Agarwal A, Xu C and Kotov N A 2010 *Angew. Chem. Int. Ed.* **49** 5472–5
[17] Marzbanrad E, Hu A, Zhao B and Zhou Y 2013 *J. Phys. Chem.* C **117** 16665–76
[18] Erb R M, Son H S, Samanta B, Rotello V M and Yellen B B 2009 *Nature* **457** 999–1002
[19] Biswal S L and Gast A P 2004 *Phys. Rev.* E **69** 041406
[20] Ding T, Song K, Clays K and Tung C 2009 *Adv. Mater.* **21** 1936–40
[21] Jalani G, Lee S, Jung C W, Jang H, Choo J and Lim D W 2013 *Analyst* **138** 4756–9
[22] Shi C, Zhang Y, Gu C, Seballos L and Zhang J Z 2008 *Nanotechnology* **19** 215304
[23] Zhang Y, Gu C, Schwartzberg A M, Chen S and Zhang J Z 2006 *Phys. Rev.* B **73** 165405
[24] Ahlawat S, Dasgupta R and Gupta P K 2008 *J. Phys. D: Appl. Phys.* **41** 105107
[25] Maragò O M *et al* 2010 *Proc. of SPIE* **7762** 77622Z
[26] Seol Y, Carpenter A E and Perkins T T 2006 *Opt. Lett.* **16** 2429–31
[27] Hallock A J, Redmond P L and Brus L E 2005 *Proc. Natl Acad. Sci.* **102** 1280–4
[28] Hu A, Rybachuk M, Lu Q B and Duley W W 2007 *Appl. Phys. Lett.* **91** 131906
[29] Hu M, Chen J, Li Z Y, Au L, Hartland G V, Li X, Marqueze M and Xia Y 2006 *Chem. Soc. Rev.* **35** 1084–94
[30] Sannomiya T and Vörös J 2011 *Trends Biotechnol.* **29** 343–51
[31] Peng P, Hu A and Zhou Y 2012 *Appl. Phys.* A **108** 685–91
[32] Israelachivili J N 2011 *Intermolecular and Surface foreces* (Amsterdam: Elsevier) pp 71–166
[33] Peng P, Huang H, Hu A, Gerlich A P and Zhou Y N 2012 *J. Mater. Chem.* **22** 15495–9
[34] Garnet E C, Cai W, Cha J J, Mahmood F, Connor S T, Christoforo M G, Cui Y, McGehee M D and Brongersma M L 2012 *Nat. Mater.* **11** 241–9
[35] Huang H, Liu L, Peng P, Hu A, Duley W W and Zhou Y 2012 *J. Appl. Phys.* **112** 123519
[36] Hutter E and Fendler J H 2004 *Adv. Mater.* **16** 1685–706
[37] Haiss W, Thanh N T K, Aveyard J and Fernig D G 2007 *Anal. Chem.* **79** 4215–21
[38] Zhou W and Odom T W 2011 *Nat. Nanotechnology* **6** 423–7
[39] Besner S, Kabashin A V and Meuniera M 2006 *Appl. Phys. Lett.* **89** 233122
[40] Link S, Burda C, Nikoobakht B and El-Sayed M A 2000 *J. Phys. Chem.* B **104** 61–3
[41] Liu L, Peng P, Hu A, Zou G, Duley W W and Zhou Y 2013 *Appl. Phys. Lett.* **102** 073107
[42] Hu A, Peng P, Alarifi H, Zhang X Y, Guo J Y, Zhou Y and Duley W W 2012 *J. Laser Appl.* **24** 042001
[43] Feng F, Zhi G, Jia H S, Cheng L, Tian Y T and Li X J 2009 *Nanotechnology* **20** 295501
[44] Xu H and Kall M 2002 *Phys. Rev. Lett.* **89** 246802